대한설비공학회 2009 하계학술발표대회 논문집 pp. 1513 ~ 1520

09-R-012

왕복동식 압축시스템에 연결된 파이프 내부의 유동특성에 관한 CFD와 실험

라 흐 만, 이 경 환, 이 광 성, 정 한 식*, 정 효 민*†
경상대학교 대학원 정밀기계공학과, *경상대학교 정밀기계공학과 해양산업연구소

CFD and Experimental Study of Gas Flow Inside the Steel Pipe Fitted in Reciprocating Hydrogen Compression System

Mohammad-Shiddiqur Rahman, Gyeong-Hwan Lee, Kwang-Sung Lee, Han-Shik Chung* and Hyo-Min Jeong*†

Department of Mechanical and Precision Engineering, Gyeongsang National University, Korea
**Department of Mechanical and Precision Engineering, Gyeongsang National University, Institute of Marine Industry, Korea*

ABSTRACT: Renewability and pollutant free energy source makes hydrogen energy popular rapidly. Hydrogen gas pressure which is after passing through reciprocating compressor part has high pulsation wave form. A unit, snubber is used as compressor components to reduce the harmful pulsation waveform and to remove the impurities in the hydrogen gas. An experiment has been conducted to investigate the pulsation reduction performance of a steel pipe used in snubber system. The amplitude of pressure reduction were varied from 0.054 ~ 0.321 kPa for 10 hz to 60 hz motor speed. Compressor operation by motor with 10 to 60 hz were resulted in reduction of pressure pulsation from 16.415% to 35.151%. Pressure losses were varied from 0.001% ~ 0.759%, and pressure drop per centimeter of the steel pipe were varied from 0.0160 ~ 16.031 Pa.

Key words: Root Mean Square, snubber array, pressure characteristics, reciprocating, hydrogen compression

Nomenclature

RMS	:	Root mean square
FFT	:	Fast fourier transformation
Pin	:	Input pressure, kPa
Pout	:	Output pressure, kPa
Pred	:	Pressure reduction (%)
Ain	:	Input pressure amplitude, kPa
Aout	:	Output pressure amplitude, kPa
Ared	:	Amplitude reduction (%)

† Corresponding author
Tel.: +82-055-640-3185; fax: +82-55-644-4766
E-mail address: hmjeong@gnu.ac.kr

1. INTRODUCTION

During the last century fossil fuels became popular for their very useful properties not shared by non-conventional energy sources (such as solar). Unfortunately, fossil fuels are not renewable.[1] In addition, the pollutants emitted by fossil energy systems (e.g. CO, CO2, CnHm, SOx, NOx, radioactivity, heavy metals, ashes, etc.) are greater and more damaging than those that might be produced

by a renewable based hydrogen energy system.[2] Harmful effects on environment for fossil fuel production and consumption stress scientists towards new alternative sources. The green energy based hydrogen system can be one of the best solutions for accelerating and ensuring global stability and substantiality. Therefore, the production of hydrogen from non-fossil fuel sources and the development and application of green energy technologies are becoming crucial in this century for better transition to hydrogen economy.[3] A scenario study has been reported incorporating a complete set of new technologies (including hydrogen production) to reduce CO2 emissions by the year 2040.[4] Hydrogen production by different approaches for splitting water have been summarized by Bockris as follows: electrolysis, plasmolysis, magnetolysis, thermal approach (direct, catalytic and cyclic decomposition of water, as well as magmalysis), use of light (photosensitized decomposition using dyes, plasma induced photolysis, photoelectrolysis, photo-aided electrolysis, the indirect path towards hydrogen by photoelectrolysis: the photoelectrochemical reduction of CO2 and photovoltaic electrolysis), biocatalytic decomposition of water, radiolysis and other approaches.[5] The assertion of "hydrogen is considered a promising future fuel for vehicles" is based on three main arguments: the potential reducing greenhouse gases from the transport sector, greater energy supply security, i. e. hydrogen can be produced from many energy sources and hence the risk of shortage of supply may be reduced; the potential of zero local emissions with the use of fuel cells. The absence of hydrogen infrastructure is seen as major obstacle to the introduction of hydrogen fuel cell vehicles. A full scale hydrogen infrastructure with production facilities, a distribution network and refueling stations is costly to build. The venture of constructing a hydrogen refueling infrastructure constitutes long-term, capital-intensive investment with great market uncertainties for fuel cell vehicles. Therefore, reducing the financial risk is major objective of any long-term goal to build hydrogen infrastructure.[6]

One of the most important processes in the hydrogen gas handling is the compressing system. This process is needed in all step of hydrogen gas energy utilization: production, storage, distribution until using.[7] In addition since hydrogen will replace the role of fossil fuel, so all approach done in this field should be rewarded. In industrial application, hydrogen gas compressing system is frequently used as the transferring or storing force device. It needs to be in high pressure condition; therefore high working compressors are required. For this purpose, usually reciprocating type is used. The reciprocating compressor can generates higher pressure. There developed pressure pulsation inherently due to reciprocating compressor mechanism. It needs remove the pulsation for its harmful effects. Snubber buffer can be used to turn down to a allowable limit. In order to damp the pressure fluctuation a flat plate is inserted inside the snubber. The single snubber is not sufficient for damping fluctuation. There needs more than one snubber. Steel pipe of specific diameter and length connect the snubbers. These pipe act as cooling chamber of temperature that develope during high pressure generation. This research is taken to study the gas flow phenomena inside the steel pipe.

2. Apparatus and test procedure

Four sensor holding structures for pressure measurement were made with acryl material. The 500 mm steel pipe was attached to these sensor structures through small PVC pipe with clamp tightly. The pictorial view is like Fig. 1. The experimental set up block diagram of the

experiment is shown in Fig. 2. The setting of different parts was attached to a frame to resist vibrations. The experiment conducted by running the compressor and setting motor frequency at 20 Hz, 30 Hz, 40 Hz and 50 Hz. Pressure from two points were taken at a time. Pressure values were measured by pressure sensors amplified and recorded them using data logger in a computer.

Fig. 1 Photographic view of experimental set up.

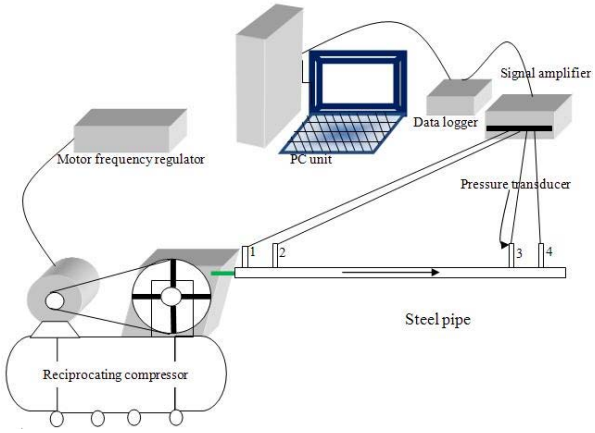

Fig. 2 Block diagram of experimental set up.

In Motor driven reciprocating pump was used in this experiment. The rotation of motor was controlled by its frequency regulator. The maximum motor rotation was 1800 rpm at maximum frequency (60 Hz). Relationship between compressor and motor pulley rotation were found as in equation 1.

$$\omega_{comp}\ [rpm\ ] = f_{set}[Hz\ ] \times 12.84\ [rpm\ /Hz\ ] \qquad (1)$$

Then piston in the cylinder will move proportionally with the rotation. The compressing frequency can be written as in equation (2).

$$f_{comp}\ [\mathrm{Hz}\ ] = f_{set}\ [\mathrm{Hz}\ ] \times 0.214 \qquad (2)$$

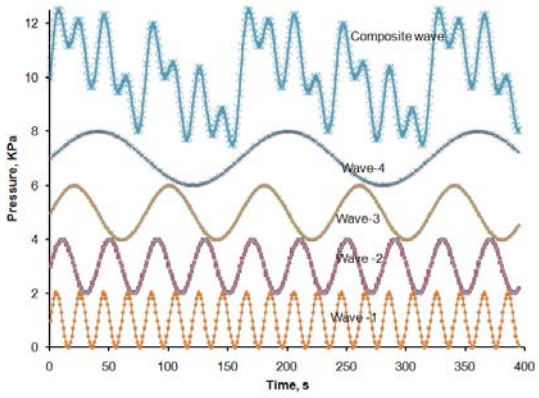

Fig. 3 Composite pressure wave.

The periodic action of propelling gas through a pipe by the to and fro movement of the piston in the cylinder in reciprocating compressor caused pulsation. The piston-crank-valve mechanism generates a variable pressure, which over time creates a composite pressure wave in the suction and discharge pipe. This composite wave is made up of a number of waves (Fig. 3). Due to periodic wave generation, multiple frequencies of pulsation are created that causes the force of vibration in the whole system.

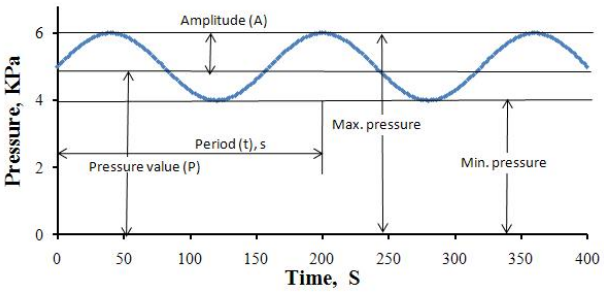

Fig. 4 Basic theory of pressure fluctuation.

Pressure produced by a piston in reciprocating compressor is fluctuating. Simple description of fluctuating notation is shown in Fig. 4. From this figure, pressure value and pressure amplitude can be derived as equation (3) and (4).

$$p = \frac{p_{max} + p_{min}}{2} \quad (3)$$

$$A = \frac{p_{max} - p_{min}}{2} \quad (4)$$

Same with the other gas line utilities, gas that passing through a snubber will be reduced in pressure and reduced in pressure fluctuation. It is related to the amplitude of pressure. The pressure reduction or loss and amplitude reduction can be expressed in the percentage by the equation (5) and (6), respectively.

$$P_{red}(\%) = \frac{P_{in} - P_{out}}{P_{in}} \times 100\,\% \quad (5)$$

$$A_{red}(\%) = \frac{A_{in} - A_{out}}{A_{in}} \times 100\,\% \quad (6)$$

Experimental data at every section were collected using data logger and analyzed them. The RMS values of input and output of pressure were used for pressure loss. FFT analysis was done to on data to find out amplitude values of the pressure waves along the snubber. The resultant value of the variables was calculated by taking square root of summation of squares of all values [8]. The pressure loss was obtained by equation (5) and the pressure pulsation reduction was calculated by equation (6) using data from experiment.

Model for simulation is made regarding the fluid passage in the steel pipe. The model was built considering the fluid area only in CATIA. The grid was generated using Pro-Surf and Pro-Am (Auto Mesh). Model was finally composed of trim cells of 12816 (Fig. 5).

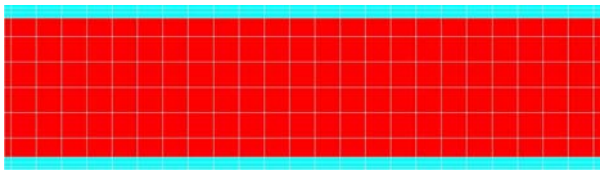

Fig. 5 Grids in steel pipe model.

The CFD solver used in this study is STAR CD version 3.24. In the present study, the 3D, unsteady state, finite volume method was used. Then the gas flow through the line can be assumed, at a very sort time, as a steady state with both inlet and outlet boundary condition. The flow also was assumed as compressible fluid. SIMPLE (Semi Implicit Method for Pressure-Linked Equations) algorithm was employed with max residual 0.001, for linked variables. Material applied was air. For turbulence modeling, k - ε high Reynolds number model, explained in mathematical model part, was used. Boundary conditions set in this study, accordingly data obtained from experiment at point 1 and point 4 which is shown in Fig. 7.

3. Results and Discussion

The Fig. 6 shows the relationship between the motor frequency and compressor frequency. When motor frequency increases compressor frequency also increase. It depends upon the diameter of the motor pulley and compressor pulley. The frequency that transformed from motor to compressor were 2.14 hz, 4.28, hz, 6.42 hz, 8.56 hz, 10.7 hz, 12.84 hz with corresponding motor frequency 10, 20, 30, 40, 50, 60 hz.

Fig. 7 is the graph showing instantaneous pressure values against times for inlet point1 and outlet point4. The pressure cycle for outlet covered 104.7004 kPa and 102.3283 kPa maximum and minimum pressure, respectively. The average inlet pressure was 103.5107 kPa. The maximum and minimum pressure were 107.8629 kPa and 102.7823 kPa for inlet

pressure of the pipe. The average 104.9275 kPa was found in the inlet for 50 hz.

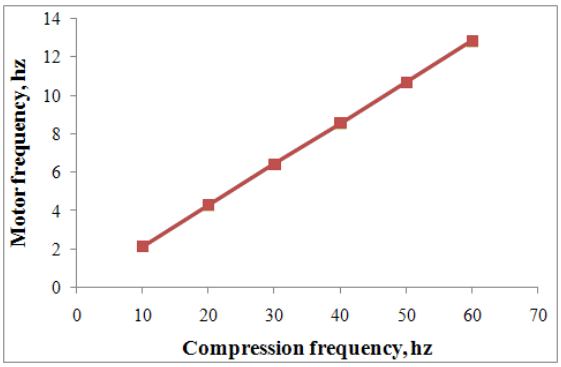

Fig. 6 Relationship between motor frequency and compressor frequency.

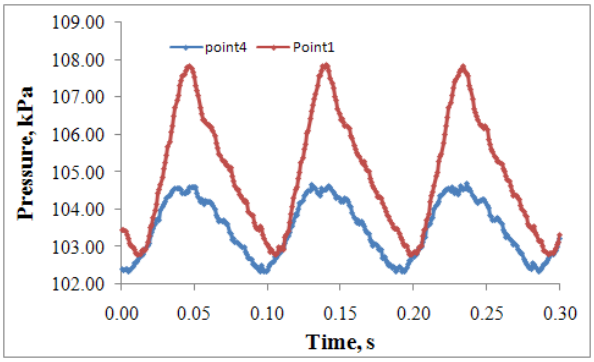

Fig. 7 Pressure in the pipe at inlet and outlet for 50Hz [P1&P4].

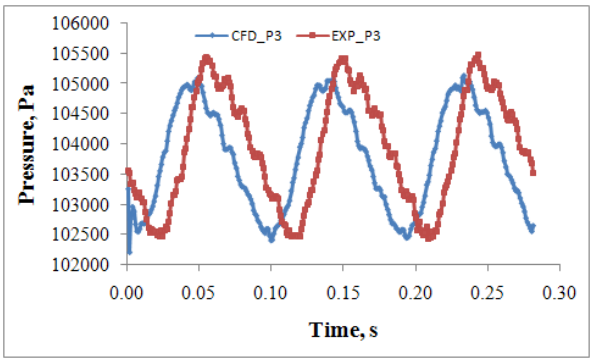

Fig. 8 Comparison of pressure between CFD and experimental at point 3 for 50 hz.

As can be seen in Fig. 8, three peaks of each experimental and simulation pressure are presented. The trend of the simulated pressure was similar. The maximum and minimum values were almost same and the intermediate small peaks are also found in simulation results. At point 3 the experimental pressure had peaks like 105419, 105412, 105412 Pa where as CFD simulated corresponding pressure peaks were 105039, 105058, 105108 Pa.

The measured pressure and simulated pressure were compared at point 2 (Fig. 9). There it is shown that the best match between them with little difference. The experimental unsteady pressure follows the route along with 102902, 102886, 102773 Pa three minimum peaks and 107273, 107313, 107302Pa three maximum peaks. The superimposing the two curve it can be concluded that the CFD simulated pressure can be accepted.

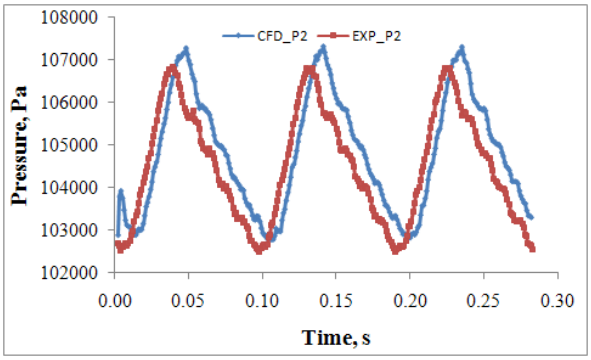

Fig. 9 Comparison between experimental and CFD simulation at point 2 for 50 hz.

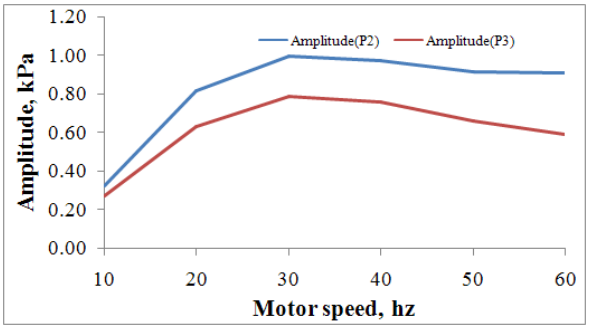

Fig. 10 Amplitude pressure at the two ends of the pipe.

After FFT calculation, the fluctuation of pressures at different speed were arranged as in Fig. 10. Compressor generates 0.327, 0.814, 0.997, 0.971, 0.915, 0.912 kPa at point 2 and 0.273, 0.632, 0.789, 0.762, 0.663, 0.592 kPa at

point 3 for the speed 10, 20, 30, 40, 50, 60 hz. It had positive relations with speed that forms curve. The harmful amplitudes drop in the steel pipe were varied with speed from 1.0740, 3.640, 4.161, 4.1813, 5.053, 6.413 Pa/cm. The percentage of amplitude reduction for 10, 20, 30, 40, 50, and 60 hz were 16.415, 22.342, 20.857, 21.529, 27.605, 35.151% in the 13mm diameter 500 mm steel pipe. It had not specific pattern but increasing trends.

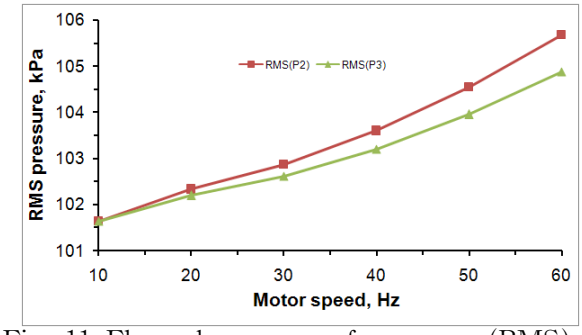

Fig. 11 Flow phenomena of pressure (RMS) at the two ends of the pipe.

Fig 11 contains the RMS values of pressure in the 500 mm steel pipe corresponding to different motor speed for compression of air in reciprocating compressor. RMS pressure for point2 forms almost straight line as the motor speed increase from 10 hz to 60 hz it was similar pattern for point 2 but less in straight line slopes. At point 2 10.639, 102.330, 102.870, 103.598, 104.540, 105.676 kPa RMS pressures were reported against 101.639, 102.192, 102.619, 103.192, 103.948, 104.874 kPa at point 3 as the motor run for 10, 20, 30, 40, 50, 60 hz, respectively. In the steel pipe the pressure drop due to its wall and passage and fluid flow phenomena were calculated as 0.0160, 2.765, 5.030, 8.118, 11.841, 16.031 Pa/cm for the speeds of the compressor. It had a positive correlation with the compressor speed i.e. pressure drop/cm increases with speed. Very small amount of percentages of RMS pressure loss were found in different compression speed varying from 0.001% to 0.759%.

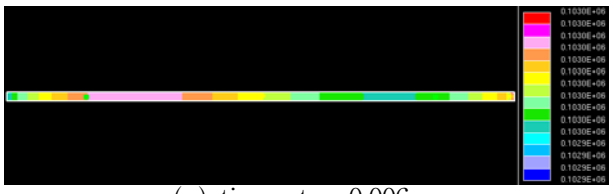
(a) time step 0.006 s.

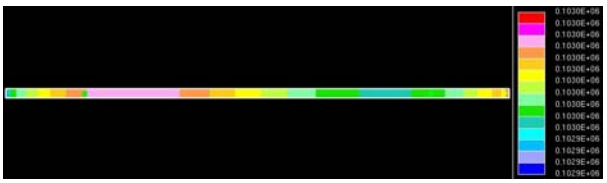
(b) time step 0.011 s.

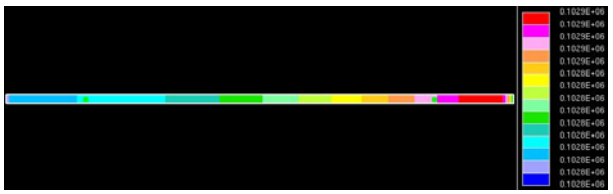
(c) time step 0.013 s.

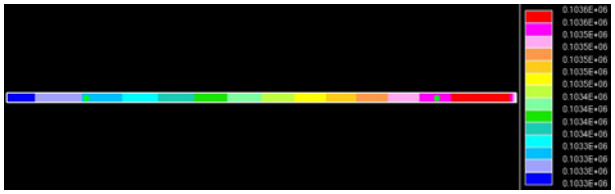
(d) time step 0.020 s.

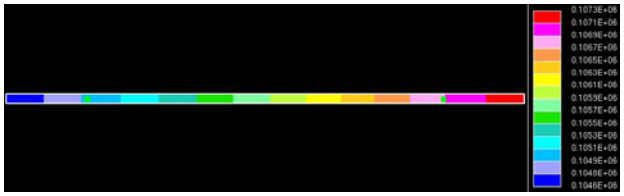
(e) time step 0.040 s.

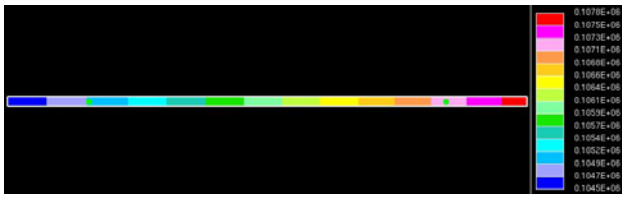
(f) time step 0.045 s.

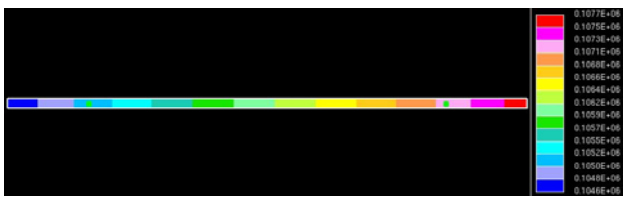
(g) time step 0.048 s.

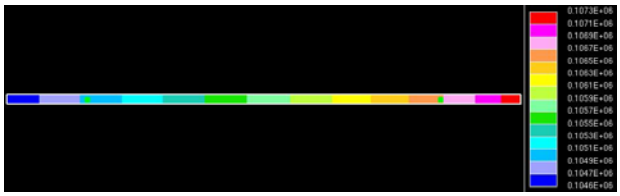

(h) time step 0.051 s.

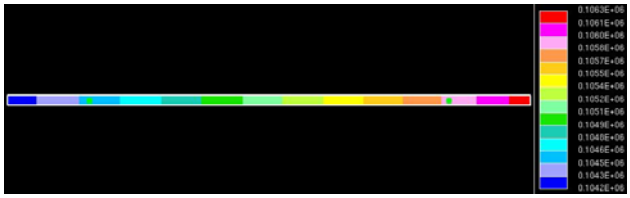

(i) time step 0.060 s.

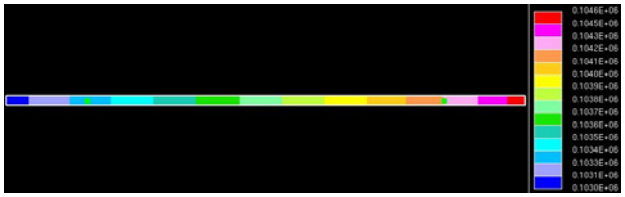

(j) time step 0.080 s.

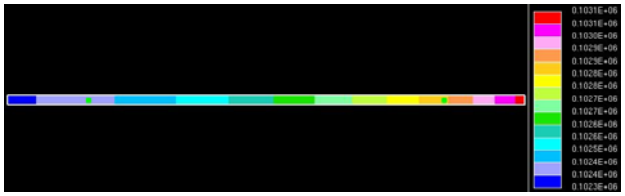

(k) time step 0.10 s.

Fig 12 Numerical pressure values at different time step covering one cycle.

Detail pressure inside the pipe at any point can be found from the numerical study. The wall pressure as well as central line pressure can also determined. Length wise or radially pressure and velocity are readily available for observation. The pressure along the length in central line are shown here in detail in the Fig 12.

4. CONCLUSIONS

The 500 mm length and 13mm diameter steel pipe pressure characteristics study has shown in this experimentally and numerically. In brief they are:

1. The amplitude of pressure reduction were varies from 0.054 ~ 0.321 kPa. Compressor operation by motor with 10 to 60 hz were able to down the pulsation varies from 16.415% to 35.151%.
2. Pressure losses are varied from 0.001% ~ 0.759%, and pressure drop per centimeter of the steel pipe are varied from 0.0160 ~ 16.031 Pa.
3. The numerical analysis gave the flow phenomena inside the pipe clearly in details.

ACKNOWLEDGEMENT

The research was financially supported by Region Strategic Planning Project from Ministry of Knowledge Economy. The Authors would like to thank the Human Resources Training Project for Regional Innovation from the Ministry of Education, Science Technology (MEST) and Korea Industrial Foundation (KOTEF) and Brain Korea 21 Project.

REFERENCES

1. Veziroglu, TN., 1987, International Journal of Hydrogen Energy, Vol. 12, No. 99 INSPEC Compendex.
2. Winter, CJ., 1987, International Journal of Hydrogen Energy, Vol. 12, No. 99 INSPEC Compendex.
3. Midili, A. and Dincer, I., 2007, Key strategies of hydrogen energy systems for sustainability, Int J. of Hydrogen Energy, Vol. 32, pp. 511-524.
4. Okken, PA., 1992, Proceedings of the Ninth World Hydrogen Energy Conference. Paris (France), pp. 1723.
5. Bockris, JOM, Dandapani, B., Cocke, D., Ghoroghchian, J., 1985, International Journal of Hydrogen Energy, Vol. 10, No. 179, INSPEC Compendex.
6. Forsberg, P. and Karlstrom, M., 2007, On optimal investment strategies for a hydrogen refueling station, Int J. of

Hydrogen Energy, Vol. 32, pp. 647-660.
7. Heever, S. A. and Grossman, I. E., 2003, A strategy for the integration of production planning and reactive scheduling in the optimization of hydrogen supply network. Journal of Computers and Chemical Engineering, Vol. 27, pp. 1831-1839.
8. Origin Lab. Co., 2003, Origin Reference v7.5. FFT Mathematical Description.